![AIAA logo]

03- 533

AIAA 97-1580

Response of High Subsonic Jet to Nonaxisymmetric Disturbances

A. Bayliss
Northwestern University
Evanston, IL

L. Maestrello
NASA Langley
Hampton, VA

3rd AIAA/CEAS
Aeroacoustics Conference
May 12-14, 1997, Atlanta, GA

RESPONSE OF HIGH SUBSONIC JET TO NONAXISYMMETRIC DISTURBANCES

A. Bayliss *

Northwestern University, Evanston, IL 60208

L. Maestrello †

NASA Langley Research Center, Hampton, VA 23681-000

Abstract

A model of sound generated in a high subsonic (Mach 0.9) circular jet is solved numerically in cylindrical coordinates for nonaxisymmetric disturbances. The jet is excited by transient mass injection by a finite duration pulse via a modulated ring source. The nonaxisymmetric solution is computed for long times after the initial disturbance has exited the computational domain.

The long time behavior of the jet is dominated by vorticity and pressure disturbances generated at the nozzle lip and growing as they convect downstream in the jet. These disturbances generate sound as they propagate. The primary nonaxisymmetric effect that we simulate is that of a flapping mode where regions of high and low pressure alternate on opposite sides of the jet. The predominant feature of this mode is the appearance of relatively large deviations of the pressure from the ambient pressure on opposite sides of the jet and the convection of these regions downstream.

We illustrate flow field, near field and far field data. Important nonaxisymmetric characteristics of the near and flow field disturbances include roughly periodic pressure elevations and depressions at opposite values of the azimuthal angle ψ. These correspond to pressure disturbances propagating in the axial direction. The azimuthal velocity exhibits a sinusoidal dependence on ψ with similar roughly periodic disturbances. For every azimuthal angle ψ the jet radiation peaks about 30° from the jet axis, however there is now a pronounced dependence of the far field radiation pattern on ψ.

*Professor, Dept. of Eng. Sciences & Appl. Math.
†Senior Staff Scientist, Associate Fellow AIAA

1 Introduction

In this paper, the generation and propagation of sound in a high subsonic jet excited by nonaxisymmetric disturbances is simulated. We consider a circular jet exiting from a straight nozzle extending to infinity in the upstream direction. The jet is excited by a nonaxisymmetric transient source and the long time behavior of the pressure is considered. We consider the full nonlinear Euler equations in conservation form modified so that a spreading jet profile, obtained from experimental measurements, is a solution in the absence of any disturbances.

The primary objectives are (i) to characterize nonaxisymmetric aspects of the flow field and near field and (ii) to characterize nonaxisymmetric effects in the far field. The jet is initially excited by a spatially and temporally localized source of transient mass injection. In contrast to previous work we consider a modulated ring source for the excitation, thus generating a nonaxisymmetric disturbance field. This leads to an initial acoustic disturbance which propagates through the jet. As a result of the excitation instability waves are generated in the jet. These waves grow and then decay as they convect downstream, generating sound in the process. This phenomenon occurs over time scales much longer than that of the excitation pulse. The emphasis in this paper is on the long time response of the jet, after the wave due to the excitation pulse has exited the domain of interest. Thus, instability wave generated sound in the jet is simulated. The simulation does not directly account for sound generated by small scale turbulent sources in the jet.

In previous work we have considered jet acoustics for circular jets subject to axisymmetric disturbances. In particular, both linear and nonlinear responses have been considered [1, 2, 3] In these references the jet is excited by a source of transient mass injection and the development of instabilities

together with associated sound generation is computed. The results in these references demonstrate the properties of instability wave generated sound. A succession of disturbances is generated at the nozzle lip. These disturbances initially grow as they convect in the jet. As they grow they generate pressure disturbances which propagate into the far field as sound. The far field radiation peaks at about 30° from the jet axis in agreement with measurements and observations.

We have also considered two dimensional Cartesian jets.[4, 5, 6, 7] In two dimensions we have computed both the sound generated from instability waves and the interaction of this sound with a nearby flexible structure. These computations spanned a range of jet velocities up to and including supersonic jets. The two dimensional results for high subsonic jets (the parameter range considered here) indicated that the long time behavior of the excited jet is dominated by a nearly periodic acoustic response at a particular fundamental frequency together with harmonics.[6] This radiation is beamed at approximately 30° from the jet axis. The unsteady flow field is dominated by disturbances generated at the nozzle lip and propagating along the jet. In contrast to the nearly periodic far field the flow field exhibited an aperiodic, apparently chaotic behavior.

The exact sources of jet noise have been identified from the basic equations of fluid dynamics.[8, 9, 10, 11, 12] Computation of the exact sources would require solution of the Navier-Stokes equations in the jet accompanied by an appropriate turbulence model. Such computations are difficult to conduct, particularly in 3 dimensions. Both small scale and large scale disturbances in the jet can act as sources of sound. In this paper we consider only sound generated from large scale instability waves. These instability waves are generated within the transiently excited jet by the mechanism described above.

Instability waves or large scale structures which can act as sources of sound in a jet have been observed in experiments[1, 13, 14] and studied by analytical[15, 16, 17, 18, 19, 20, 21] and numerical[1, 1, 3, 22] methods. While there have been a limited number of 3 dimensional computations [23, 24], the cost of the 3D computations has to date precluded a detailed study of the role of nonaxisymmetric large scale structures as sources of jet noise and has generally forced restrictive assumptions such as linearity. On the other hand, many of the large scale structures observed in experiments are intrinsically nonaxisymmetric, e.g., flap-

ping modes where regions of large pressure alternate on different sides of the jet, and thus a full understanding of jet acoustics requires an understanding of nonaxisymmetric modes in the jet and the resulting acoustic radiation.

In our model we solve a modified version of the full nonlinear Euler equations in cylindrical geometry. The equations are modified to account for a spreading jet as described below. As a result, the inviscid, instability wave sources of sound are computed directly together with the resulting sound generation. We specifically include a straight nozzle from which the jet exits. The flow field and near field disturbances are computed together with the far field sound radiation.

2 Model and Numerical Method

The computational domain is shown in Figure 1. We consider a jet exiting from a straight, circular pipe of diameter D, where $D = 4$ inches. All boundaries are artificial boundaries at which radiation boundary conditions are employed.[1, 27] The jet is excited by a transient source of mass injection located approximately $1D$ downstream from the nozzle exit. This source is both spatially and temporally localized, leading to a broad band excitation. Unsteady pressure, density and velocity are computed both interior and exterior to the pipe. This leads to the generation of a train of instability waves which propagate along the jet, decaying beyond the potential core of the jet and generating sound.

The Euler computations employ a (2-4) version of the MacCormack scheme.[25] Further details on the numerical scheme are given in the references.[4, 5, 6] The spatial fourth order accuracy is necessary in order to follow the acoustic waves over large distances without undue numerical dispersion. This is particularly important given the coarse grids necessitated by nonaxisymmetric computations.

The Euler equations are solved in conservation form in cylindrical coordinates z, r, ψ, where z denotes the axial distance, r the radial distance and ψ is the azimuthal angle. The dependent variable is the vector

$$\hat{q} = (\rho, \rho u, \rho v, \rho w, E)^T,$$

where ρ is the density, u, v and w are the axial, radial and azimuthal velocity components respectively, and E is the total energy per unit volume. The pressure, p, is obtained from the equation of state.

The Euler equations are modified in the jet domain to account for the jet flow. The jet exits from a nozzle of diameter D located at $z = 0$ and the

solution is computed both within and exterior to the nozzle. The Euler equations are modified to account for two different non-homogeneous forcing terms.[6] One term serves as an excitation pulse to excite the jet. It corresponds to a localized source of mass injection. In axisymmetric computations we take a point source centered on the axis at z_s. In the nonaxisymmetric computations we consider a ring source of radius r_s, where $r_s \simeq .3D$. For each ψ the source is a peaked Gaussian centered at r_s, z_s. In order to obtain a nonaxisymmetric excitation the strength of the source is modulated by the function $1 + \epsilon \cos \psi$, where $\epsilon = 0.2$. The temporal dependence of the source is described in the references, e.g., [4]. The source is localized in time leading to broad band excitation.

The second forcing term is designed so that in the absence of the excitation pulse the solution to the Euler equations would be a stationary profile corresponding to a spreading jet. In the present computation, mean density and pressure are assumed constant, as are the mean radial and azimuthal velocities. The mean axial velocity U is a taken from experimental measurements and models an isothermal jet with exit Mach number 0.9. [26]

The inclusion of this term separates the computation of the disturbance, in particular the resulting instability waves, from the computation of the mean flow (i.e. the spreading jet). Thus, the resulting system of equations allows for the simulation of instability waves and the resulting sound generation, together with the propagation of acoustic waves in the jet flow field, without requiring the computation of the spreading jet itself. Although this is a simplified model, it captures many of the observed features of instability wave generated jet sound and permits high resolution computation of the coupling of jet noise with the flexible panels and the resulting radiation from the panels. In particular, the model allows for computation of many of the natural sources of jet noise (the instability waves) together with the sound radiated by these sources.

3 Numerical Results

The primary objective of the computations is to examine flapping modes, in which regions of high pressure in the jet alternate at opposite azimuthal angles. We consider the unsteady pressure $\bar{p} = p(t, r, z, \psi) - p_\infty$ where p_∞ is the ambient pressure. In response to the excitation source an initial acoustic wave emanates from the source location through the jet. In addition, a large slowly moving structure, an instability wave, propagates

downstream along the jet axis. We consider the transient effects. We concentrate on the long time behavior of the jet which is dominated by a shedding of disturbances from the nozzle lip, the propagation of these disturbances downstream and the generation of sound from these disturbances as they grow and decay along the jet. We note that there are also disturbances that propagate upstream inside the pipe.

In Figure 2 we consider color contours for $\bar{p}$ in the $r - z$ plane $\sin(\psi) = 0$, i.e., the pressure field for the angles $\psi = 0$ and $\psi = \pi$. The coloring is according to the spectrum with red indicating large positive values of $\bar{p}$ and violet indicating large negative values of $\bar{p}$. Note that colors are assigned based on a logarithmic scale. These contours are shown in Figure 2 at 6 different times, $t_1, \ldots, t_6$, where the nondimensional time t is defined by $t = \bar{t} U_e / D$, $\bar{t}$ is dimensional time and U_e is the jet exit velocity. The times illustrated in Figure 2 are $t_1 = 28.08$, $t_2 = 29.19$, $t_3 = 30.83$, $t_4 = 31.93$, $t_5 = 33.02$, $t_6 = 33.56$.

Note that these figures show only a portion of the larger computational domain, which extends $30D$ both upstream and downstream of the nozzle exit and radially. In interpreting these figures, we recall that the nozzle exit is at $z = 0$ and the initial source was a ring source centered approximately $1D$ downstream of the nozzle exit and of approximately $0.5D$ in radius.

For each time there is an array of acoustic waves propagating primarily upstream and emanating from disturbances near the nozzle exit. In addition, large radiation, predominantly yellow in color can be seen emanating at mid angles from the jet. Note that the mid angle radiation is of greater spatial extent than the upstream radiation, indicating a low frequency, relatively broad band spectrum at mid angles and a higher frequency, sharper spectrum radiation field at upstream angles. In addition, the propagation of disturbances up the nozzle can be clearly seen. The flapping mode is best visualized by the alternating regions of large radiation (yellow) emanating from disturbances in the jet. At times t_1 and t_2 this radiation is most pronounced in the lower half of the figure ($\psi = \pi$), whereas for times $t_3 - t_6$ the predominant near field pressure disturbance is in the upper portion of the figure ($\psi = 0$). As time evolves these pressure disturbances propagate into the far field and weaken due to spherical decay. Thus, for example, the $\psi = 0$ yellow disturbance seen at approximately $2D$ downstream at t_1 becomes the yellow-green disturbance at approximately $5D$ downstream at t_2 while a yellow distur-

bance has been generated in the lower half of the figure ($\psi = \pi$) figure at approximately $2D$ at time t_3. A similar effect is seen at other angles, although the greatest contrast is for the $\psi = 0/\psi = \pi$ plane, which is also the plane of the largest asymmetry of the excitation source. Note that the figure also indicates that pressure disturbances emanating from the shear layer become coupled with the rigid pipe as they propagate outward. The coupling switches from top to bottom as the disturbances in the shear layer switch.

Another perspective of this flapping is shown in Figure 3 where pressure in a cross section of constant z/D is shown at 6 different times, $t_a, \ldots, t_f$. Here, $t_a = 22.61$, $t_b = 24.26$, $t_c = 24.80$, $t_d = 27.00$, $t_e = 28.09$ and $t_f = 33.02$. The cross section is taken at the axial location $z/D = 4.89$ just before the end of the potential core of the jet. The diameter of each cross section is approximately $2D$, the coloring is again according to the spectrum, and, due to the wide range of values involved, for each time the data is internally scaled. For each of cross section $\psi = 0$ corresponds to the right horizontal axis while $\psi = \pi$ corresponds to the left horizontal axis. Thus, at times t_a and t_b there is high pressure near $\psi = \pi$ for this particular axial location, while at times t_e and t_f the high pressure occurs near $\psi = 0$. From Figure 2, it can be inferred that there are disturbances with high pressures alternating between $\psi = 0$ and $\psi = \pi$ shed from the nozzle lip and propagating downstream along the jet. It can also be seen from Figure 3 that the solution is symmetric with respect to reflections across the horizontal axis in the cross section, i.e., under the transformation $\psi \rightarrow -\psi$. The nonaxisymmetric source distribution exhibits this symmetry and it appears to be maintained by the solution.

We next examine the flow field azimuthal velocity w. We consider w as a function of ψ at a particular flow field location near the edge of the jet shear layer. In Figure 4, w is plotted as a function of ψ for a range of values of t (after the large instability wave has passed this point). The data is taken at approximately 3,5 diameters downstream and inside the jet flow ($r/D = 0.7$). It can be seen from the figure that as a function of ψ, w exhibits a cosine dependence (inherited from the initial nonaxisymmetric disturbance) together with ripples that appear at roughly equally spaced intervals in time. These ripples represent local maxima and minima of w in time and are associated with a succession of flow field disturbances generated at the nozzle lip and convecting downstream in the jet (these disturbances can also be seen in Figure 2). It appears that the angular

locations of these ripples (i.e., of the maxima and minima of disturbances passing a fixed point) undergoes a slow rotation in ψ as can be seen from the lines drawn on the figure.

In Figures 5a and 5b we examine $\bar{p}$ outside of the flow field at a distance $6D$ from the source center. Examination of points at greater distances from the source center indicates that this figure qualitatively represents far field acoustic pressure. In Figure 5a, $\bar{p}$ is plotted against t for points at 30° from the jet axis for $\psi = 0$ and $\psi = \pi$. Figure 5b is similar except that it is for points at 90° from the jet axis. Both figures use data only for times after the leading acoustic pulse has passed the given points.

The figures at both points illustrate the effect of the near and flow field flapping on the far field pressure. Note in particular the alternating intervals in which the angular location of the larger values of $\bar{p}$ switches from $\psi = 0$ to $\psi = \pi$. The figure illustrates that the timescale of the switching is generally greater than the timescales associated with the oscillations in $\bar{p}$ as t varies. Furthermore, the figures illustrate the larger radiated pressure at mid angles as opposed to upstream or vertical angles. Finally, the figures illustrate the predominant low frequency beaming at mid angles (alternatively the preferred beaming of high frequencies upstream and at vertical angles).

In Figure 6 we exhibit the power spectral density (PSD) for $\bar{p}$ plotted against Strouhal number, $s_t = fD/U_e$, where f is the frequency for a fixed location in the flow field. Specifically, we consider $\bar{p}$ at the point $z/D = 1.1$, $r/D = 0.5$ and $\psi = 0$ which is in the shear layer of the jet. The PSD is taken over a window which excludes the initial pulse. The figure shows that most of the spectral energy is concentrated in a Strouhal number band between 0.3 and 0.6. This is a higher range than the peak radiation observed in the far field, indicating that high frequency disturbances in the flow field are not necessarily efficient radiators of sound. Note that the PSD exhibits 2 distinct peaks at apparently incommensurate frequencies, a result contrary to that found for 2 dimensional Cartesian jets with a similar Mach number where the flow field pressure exhibited narrow peaks at one particular frequency together with harmonics.[6] We also note the similarity between Figure 6 and measured spectra in nonaxisymmetrically excited jets.[28] At this point in time we have not as yet conducted a systematic investigation of the spectra at other points in the flow field.

4

4 Conclusion

We have developed a code to solve the nonlinear Euler equations for nonaxisymmetric disturbances in an axisymmetric jet. The code is second order in time and fourth order in space and is written in cylindrical coordinates with the cylindrical axis the axis of the jet. The simulation includes both the near and far field of the jet as well as the upstream region including a straight pipe from which the jet exits. The jet is excited by a transient, non-axsymmetric ring source located near the nozzle exit. The long time behavior of the jet is dominated by a train of disturbances generated at the nozzle lip and propagating downstream along the jet. These disturbances in turn generate sound as they grow and decay in the jet shear layer.

The primary nonaxisymmetric feature that we have studied is a flapping mode of propagation within the jet. In these modes regions of high pressure switch 180° at certain time intervals. These intervals are generally long compared to the timescales of oscillation of the pressure within and outside of the jet. The flapping is also apparent in the pressure outside of the jet.

There is a significant beaming of low frequency sound at mid angles to the jet axis, leading to an overall peak in the sound pressure level. In contrast, high frequencies are beamed predominantly at angles of 90° and greater to the jet axis.

The unsteady pressure in the jet flow field is primarily concentrated within the Strouhal number band between 0.3 and 0.6. Within this band there are 2 incommensurate spectral peaks. This is in contrast to results for 2 dimensional Cartesian jets where narrow peaks at a particular frequency and its harmonics are observed.

Acknowledgments

References

[1] Maestrello, L., Bayliss, A. and Turkel, E., "On the Interaction of a Sound Pulse with the Shear Layer of an Axisymmetric Jet," *Journal of Sound and Vibration*, Vol. 74, 1981, pp. 281-301.

[2] Maestrello, L. and Bayliss, A., "Flowfield and Far Field Acoustic Amplification Properties of Heated and Unheated Jet," *AIAA Journal* Vol. 20, 1982, pp. 1539-154 .

[3] Bayliss, A., Maestrello, L. and Turkel, E., "On the Interaction of a Sound Pulse With the Shear Layer of an Axisymmetric Jet, III: Non Linear Effects," *Journal of Sound and Vibration*, Vol. 107, 1986, pp. 16 -175.

[4] McGreevy, J.L., Bayliss, A. and Maestrello, L. "Interaction of Jet Noise with a Nearby Panel Assembly," *AIAA Journal*, Vol. 33, 1995 pp. 577-585.

[5] Bayliss, A., Maestrello, L., McGreevy, J.L. and Fenno, C.C., "Forward Motion Effects on Jet Noise, Panel Vibration, and Radiation," *AIAA Journal*, Vol. 34, 1996, pp. 103-1110.

[6] Fenno, C.C., Bayliss, A. and Maestrello, L. "Panel-Structure Response to Acoustic Forcing by a Nearly Sonic Jet," *AIAA Journal*, Vol. 35 1997, pp. 219-227.

[7] Fenno, C.C., Bayliss, A. and Maestrello, L., "Interaction of Sound From Supersonic Jets With Nearby Structures," AIAA paper 97-0283, 35th Aerospace Sciences Meeting, Reno, NV, January, 1997.

[8] Lighthill, M.J., "On Sound Generated Aerodynamically-I, General Theory," *Proceedings of the Royal Society*, Vol. A22 , 1954, pp. 1-32.

[9] Lilley, G.M., "Theory of Turbulence Generated Jet Noise: Generation of Sound in a Mixing Region," *U.S. Air Force Technical Report AFAPL-TR-72-53, IV*, Wright Patterson AFB, 1972.

[10] Ribner, H.S., "Dryden Lecture, Perspectives on Jet Noise," *AIAA Journal*, Vol. 19, 1981, pp. 1513-1526.

[11] Ribner, H.S., "Effects of Jet Flow on Jet Noise Via an Extension to the Lighthill Model," J. Fluid Mech., Vol. 321, 1996, pp. 1-24. NASA Technical Memorandum 110163, 1995.

[12] Ffowcs Williams, J.E. and Kempton, A. J., "The Noise from the Large-Scale Structure of a Jet," *J. Fluid Mech.*, Vol. 34, 1975, pp. 673-694.

[13] Crow, S. and Champagne, F., "Orderly Structure in Jet Turbulence," *Journal of Fluid Mechanics*, Vol. 48, 1971, pp. 4 7-591.

[14] McLaughlin, D. K., Morrison, G.L. and Trout, T.R.,"Reynolds Number Dependence in Supersonic Jet Noise," *AIAA Journal*, Vol. 15, 1977, pp. 526-532.

[15] Bechert, D.W. and Pfizenmaier, E., "On the Amplification of Broadband Jet Noise by Pure Tone Excitation," *Journal of Sound and Vibration*, Vol. 43, 1975, pp. 581-587.

[16] Huerre, P. and Monkewitz, P. A., "Local and Global Instabilities in Spatially-Developing Flows," *Annual Review of Fluid Mechanics*, Vol. 22, 1990, pp. 473-537.

[17] Monkewitz, P. A., Berger, E. and Schumm, M., "The Nonlinear Stability of Spatially Inhomogeneous Shear Flows, Including the Effect of Feedback, " Eur. J. Mech. B/Fluids, Vol. 10, No. 2, 1991, pp. 295-300.

[18] Plaschko, P. "Helical Instabilities of Slowly Divergent Jets," J. Fluid Mech. B/Fluids, Vol. 92, 1979, pp. 209-215.

[19] Strange, P., J. R, and Crighton, D. G., "Spinning Modes On Axisymmetric Jets. Part I," J. Fluid Mech. B/Fluids, Vol. 134, 1983, pp. 231-245.

[20] Michalke, A. and Hermann, G., "On the Inviscid Instability of a Circular Jet With External Flow," *Journal of Fluid Mechanics*, Vol. 114, 1982, pp. 343-359.

[21] Michalke, A., "Survey on Jet Instability Theory," *Progress in Aerospace Science*, Vol. 21, 1984, pp. 159-199.

[22] Mankbadi, R., Hayder, M. and Povinelli, L., "The Structure of Supersonic Jet Flow and Its Radiated Sound," *AIAA Journal*, Vol. 32, 1994, pp. 897-906.

[23] Hixon, R, Shih, S. H. and Makbadi, R. R., "Direct Prediction of the Three Dimensional Acoustic Field of a Supersonic Jet Using Linearized Euler Equations, " AIAA paper 95-116, June, 1995.

[24] Bangalore, A., Morris, P. J. and Long, L.,N., "A Parallel Three Dimensional Computational Aeroacoustics Method Using a Nonlinear Disturbance Equation", AIAA Paper 96-1728, May, 1996.

[25] Gottlieb, D. and Turkel, E., "Dissipative Two-Four Methods For Time-Dependent Problems,"
Mathematics of Computation, Vol. 30, 1976, pp. 703-723.

[26] Maestrello, L., "Acoustic Energy Flow From Subsonic Jets and Their Mean and Turbulent Flow Structure," Ph.D. Thesis, University of Southampton, England, UK, 1975.

[27] Bayliss, A. and Turkel, E., "Radiation Boundary Conditions for Wave-Like Equations," *Communications on Pure and Applied Mathematics*, Vol. 33, 1980, pp. 707-725.

[28] Gursul, I., "Effect of Nonaxisymmetric Forcing on a Swirling Jet with Vortex Breakdown," *Transactions of the ASME*, Vol. 118, 1996, pp. 316-321.
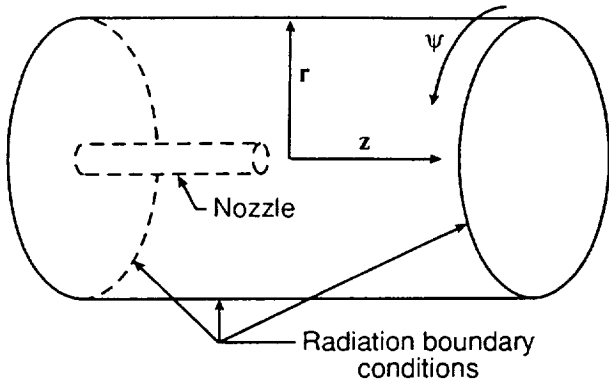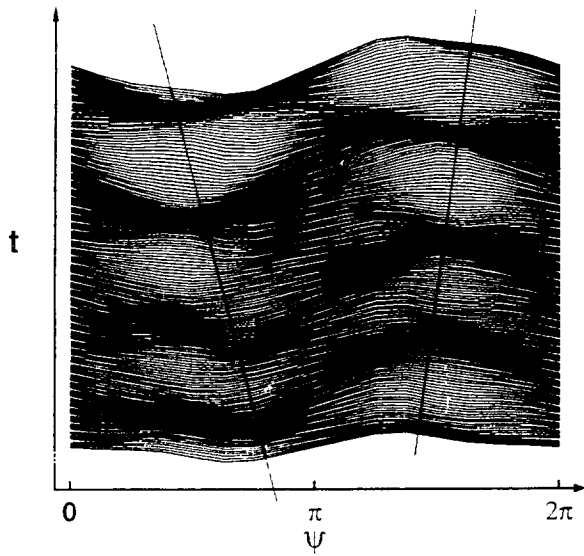
6

Figure 1. Computational domain.

Figure 5a. Far field pressure at 30 degrees from jet axis.

Figure 4. Azimuthal velocity at different times, z/D=3.5, r/D=0.7.
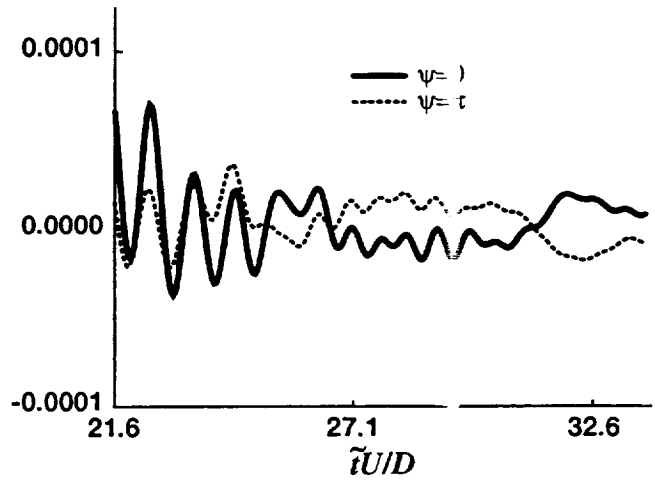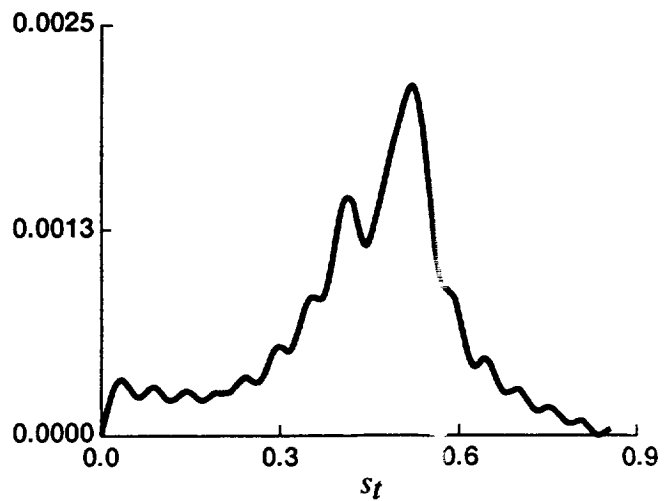

Figure 5b. Far field pressure at 90 degrees from jet axis.

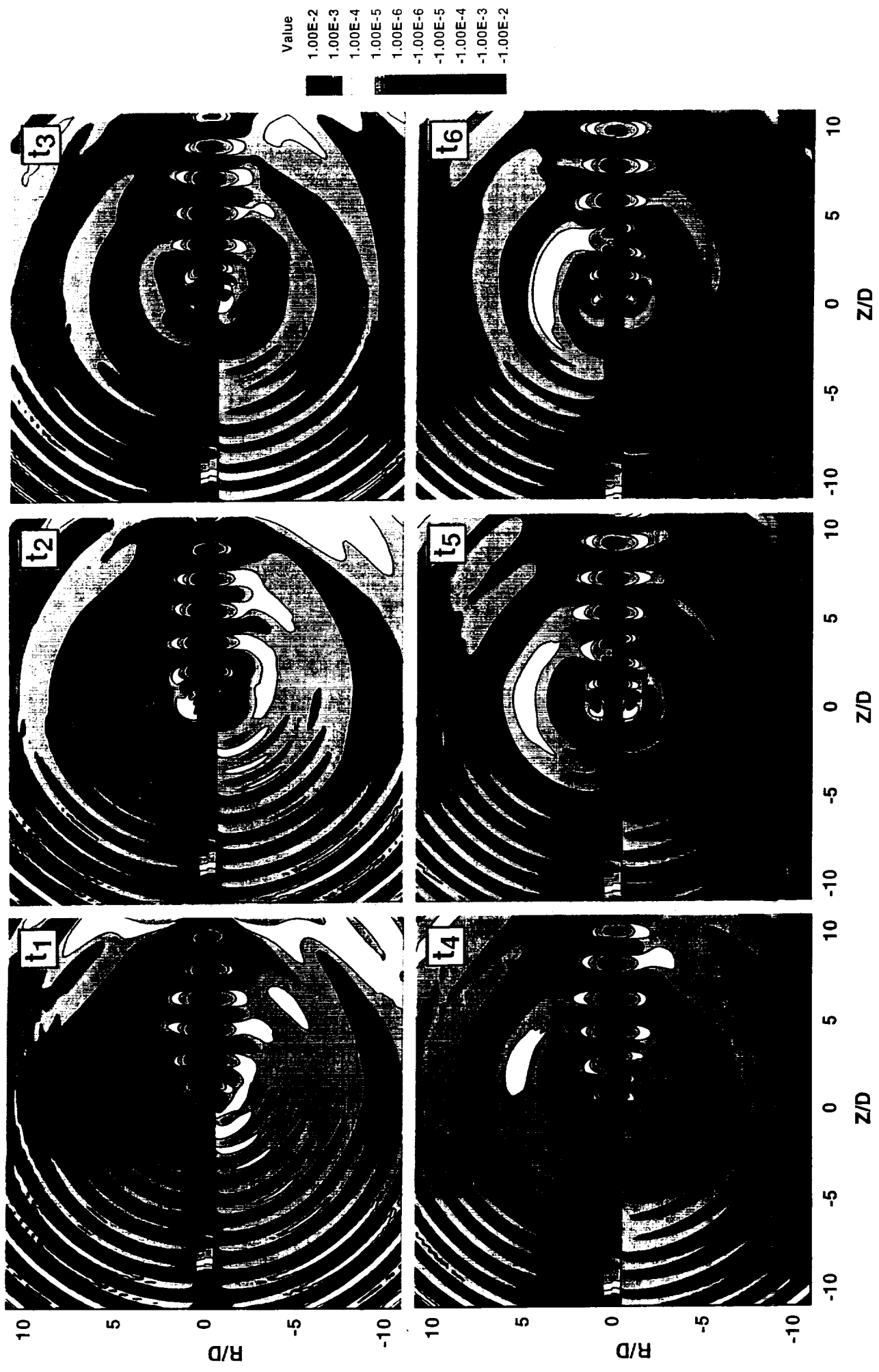Figure6. Power spectral density for $\bar{p}$ at z/D=1.1, r/D=0.5

Figure 2. Pressure contours at successive time intervals

t1 t2 t3 t4 t5 t6

Value
1.00E-2
1.00E-3
1.00E-4
1.00E-5
1.00E-6
-1.00E-6
-1.00E-5
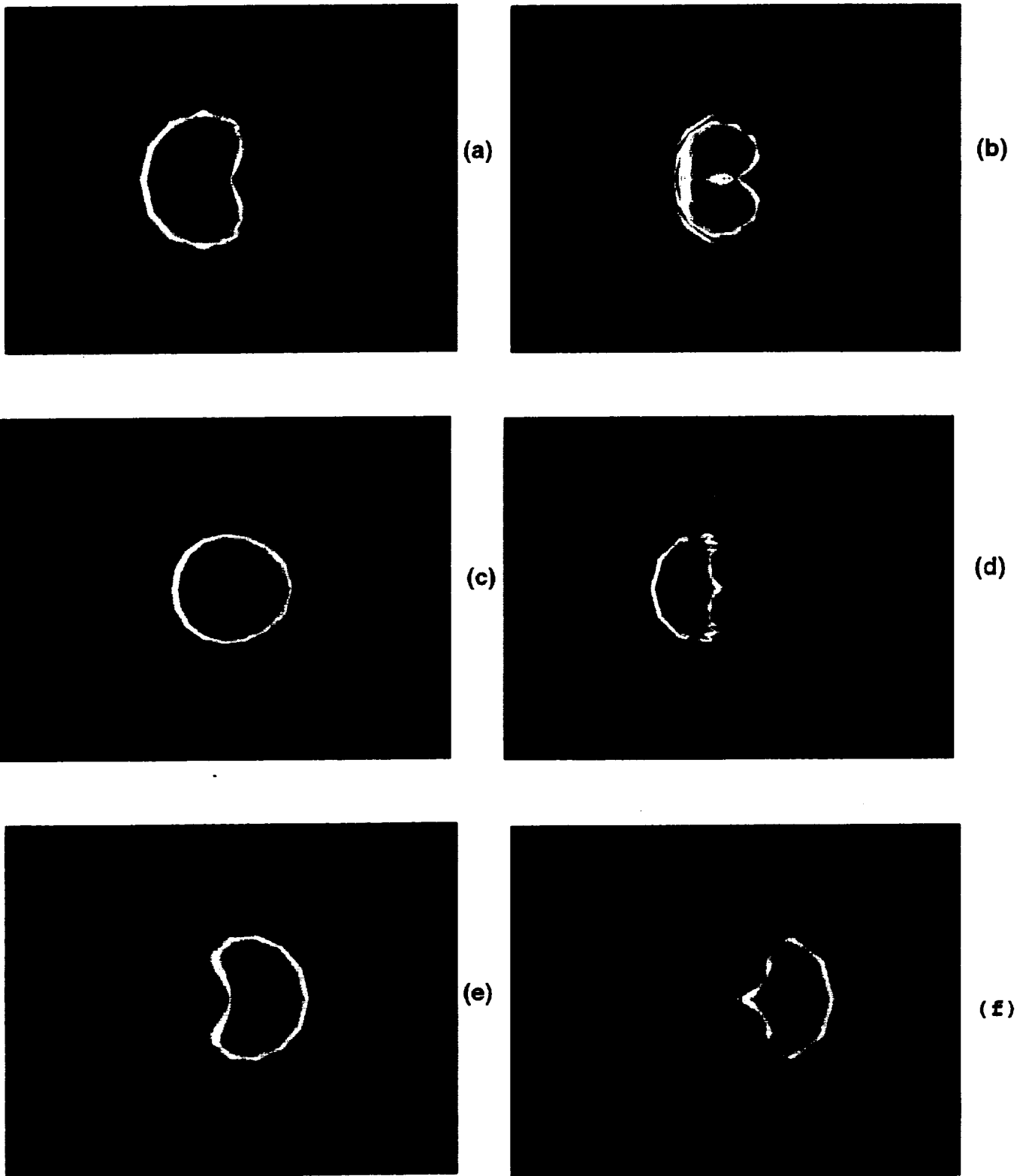-1.00E-4
-1.00E-3
-1.00E-2

R/D
Z/D

Figure 3. Visualization of pressure in jet cross section for times t_a - t_f. Axial location z/D = 4.89. Radius of each cross section is approximately 2D.